Autonomous Microgrid Restoration Using Grid-Forming Inverters and Smart Circuit Breakers

Abhishek Banerjee*, Amit Pandey*, Uttam Reddy Pailla*, Gab-Su Seo†, Shashank Shekhar*,
Himanshu Jain‡, Yashen Lin†, Xiaofan Wu*, Joachim Bamberger*, and Ulrich Muenz*
*Autonomous Systems and Control, Siemens Technology, Princeton, NJ 08540, USA
†Power Systems Engineering Center, National Renewable Energy Laboratory, Golden, CO 80401, USA
‡Department of Hydro and Renewable Energy, Indian Institute of Technology, Roorkee, India
email: {abhishek.banerjee, ulrich.muenz}@siemens.com; {gabsu.seo, yashen.lin}@nrel.gov

***Abstract*—The proliferation of distributed inverter-based resources (IBRs) raises the questions if these IBRs can be used to blackstart microgrids and distribution feeders after major outages. In this paper, we propose and evaluate an autonomous microgrid restoration concept using grid-forming (GFM) IBRs and smart circuit breakers (SCBs). The concept is first explored in simulation platform and then a hardware testbed containing actual GFM inverters is developed to demonstrate these functionalities. A combination of dispatchable virtual oscillator control (dVOC) and droop-based control schemes have been designed for GFM inverter controls in the software simulations and hardware testbed. Subsequently, operation of SCBs using two distinct principles have been demonstrated that can restore or connect portions of the network.**

***Index Terms*—Grid-forming inverters, black start, grid reconfiguration, smart circuit breaker.**

I. Introduction

With an increasing level of renewable energy resources in power systems, mostly interfaced with power electronic inverters, active use of inverter-based resources (IBR) for grid operation has been discussed [1]. Currently, most inverters deployed operate in a grid-following mode that requires grid voltage well regulated by synchronous generators. Grid-following inverters synchronize their internal reference to the grid, using a phase-locked loop in general, implying technical challenges expected in high penetration of IBRs [2].

In contrast, grid-forming (GFM) inverters can regulate their output voltage and frequency, i.e., behaving as voltage source. Most GFM approaches focus on droop control for its easier implementation and backward compatibility [2]–[4], make droop control a solution widely accepted by utilities and practitioners. Virtual oscillator control (VOC) has been proposed to improve the dynamic GFM performance while retaining the droop characteristics for compatibility [5], [6]. The *dispatchable* VOC (dVOC) adds power setpoints [7]. Similar to droop, it controls the power injections using local measurements with improved synchronization. This paper studies both GFM controls.

One emerging topic in this space is the system restoration using GFM inverters [8], [9]. Using the voltage source control embedded, the GFM inverters can establish voltage and frequency independently to form a grid in blackout if properly designed. It would be a critical functionality the new type of inverter can provide for increased grid resilience against natural disasters and cyberattacks that may cause system-wide blackout. However, it is not clear yet how to coordinate multiple inverters and microgrids, without heavy human intervention or dedicated communication involved, to facilitate the recovery process.

This paper addresses these questions with the concept of smart circuit breakers (SCB) along with GFM inverters. In the concept, control assets, i.e., inverters and SCBs, operate autonomously based on the local measurements, without communications. The GFM inverters collectively black start and maintain the grid. The SCBs interconnect sections of a grid, only with local measurements, combining microgrids and energizing local loads, to improve system reliability and achieve sustainable operation.

II. Smart Circuit Breaker for Autonomous Microgrid Reconfiguration

A major requirement for the inverter black start is the ability to reconstruct the power grid in the presence of fault conditions. After a blackout, the state of the power grid may be unknown, and communication between control devices may be limited. There may be downed lines, or faulty devices (which could have caused the blackout). It is dangerous if energization takes place in the presence of faults without any mechanism to mitigate the fault risk. To this end, SCBs can be used in conjunction with GFM inverters to achieve microgrid restoration and autonomous black start, with no or reduced reliance on the communication. An SCB is a switching device that serves several purposes, as shown in Figs. 1(a) and (b), it can detect fault conditions (e.g., short circuit or overload) and disconnect the faulty device or section from the network as

Funding provided by the U. S. Department of Energy Office of Energy Efficiency and Renewable Energy Solar Energy Technologies Office; award number DE-EE0008769. This work was authored in part by Alliance for Sustainable Energy, LLC, the manager and operator of the National Renewable Energy Laboratory for the U.S. Department of Energy (DOE) under Contract No. DE-AC36-08GO28308.

to not impede restoration. Further, as shown in Fig. 1(c), the smart switch can interconnect energized networks to improve the system reliability. It should be noted that although industry practices exist for synchronizing microgrids on different voltage levels, it aims to provide additional functionalities such as overloading detection and fault isolation that make the SCBs unique, distinguishing them from existing solutions. Although the SCB concept can be applied in various voltage and application levels, currently, the hardware microgrid testbed uses a low-voltage-rated SCB, as a proof of concept. On the other hand, the simulation systems test medium-voltage-rated SCBs modeled in software to demonstrate the scalability of the concept. The timing for closing the SCBs based on two operating principles are described further.

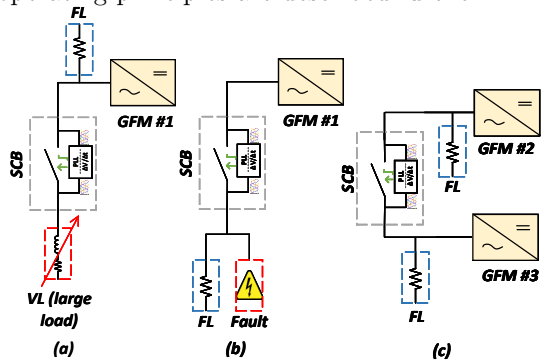

Fig. 1: Functionalities of SCBs: (a) disconnection of overload, (b) disconnection of short-circuit/fault, and (c) grid interconnection.

- **An instantaneous voltage difference-based** method monitors instantaneous difference in the two microgrid voltages to identify the closing timing. The two different microgrid voltages can be defined as:

$$\begin{aligned} v_{1,a} &= V_1 cos(\omega_1 t) \\ v_{2,a} &= V_2 cos(\omega_2 t + \theta) \end{aligned} \tag{1}$$

where $v_{1,a}$ and $v_{2,a}$ are *a-phase* voltages of microgrid #1 and #2, respectively. Since the breaker closing shorts the two different voltage domains with a small breaker impedance, the inrush current is a function of the voltages. Ideally, the circuit breaker should close when the difference is zero. However, it is not practical due to delays embedded in the relay operation. A practical method is to close the switch when the voltage difference is under a certain value to limit the inrush current. To identify the closing timing window, a mathematical derivation is presented.

With balanced three-phase voltages assumed, a voltage difference factor that captures a scaled version of the three-phase voltage differences can be defined, and a simplified form to provide intuition is derived as:

$$\begin{aligned} \kappa_v &= 0.5\left(|v_{1,a} - v_{2,a}| + |v_{1,b} - v_{2,b}| + |v_{1,c} - v_{2,c}|\right) \\ &\approx (V_1 + V_2)|sin(\pi \Delta f t)| \end{aligned} \tag{2}$$

where $\Delta f = \omega_1 - \omega_2$. The equation implies that the voltage difference will be a periodic signal with $0.5\Delta f$. With Δf large, the zero crossing would occur frequently; however, the stiffer slope forms a narrow turn-on timing window. Noting the SCB will close when κ_v is under a certain value, a further approximation can be made with $sinx \approx x$ and $V_1 + V_2 \approx 2V_{n,p}$, the peak value of the system nominal voltage: $\kappa_v \approx 2V_{n,p}\pi\Delta f t$. The equation allows for deriving a practical equation to determine the breaker closing time window:

$$T_w = \frac{K_v}{2V_{n,p}\pi\Delta f} \tag{3}$$

where K_v is a relative factor to $2V_{n,p}$, which should be determined considering the application and breaker delay.

- **A PLL based timing logic** deploys PLLs that are hosted on the micro-controller boards. Each PLL tracks the three-phase voltages, aligning internal voltage vector to each side, and yields each microgrid's d-axis voltage and phase angle. The differences of the two voltages and angles are used to determine the breaker closing timing. In a case both sides of the circuit breaker are energized, the breaker closes only when the differences in voltages (Ω) and phase angles (Δ) are less than the thresholds, V_{th} and θ_{th}, respectively. Otherwise, it is kept open. In case that only one side is energized, the circuit breaker would bypass the conditions above and attempt to close to recover the other side. If it causes a overloading, it opens and reattempts afterwards on a regular basis or may lockout as predetermined. This operation applies to both methods discussed. Table I summarizes the two methods.

TABLE I: Comparison of Smart Circuit Breaker Methods.

	Voltage difference	PLL-based
Feature	open loop	closed loop
Pros	prompt operation	add. intelligence available
Cons	filter needed for noise immunity	PLL dynamic dependent (stable voltage needed)

III. Test System Description

This section describes the test systems used to perform and test the black start and dynamic microgrid reconfiguration using the SCBs. A software platform is built on the MATLAB/Simulink environment based on the model found in [10]. The hardware testbed is a 2-bus system with 12-GFM inverters, shown in Fig.4. Although the hardware testbed operates in a lower-voltage level as compared to actual microgrids in the field, the testbed can emulate realistic conditions for testing and validation of the concept of SCB and autonomous system restoration that can be scaled up for field deployment.

A. Software Models

The IEEE 9-bus test case is modified to demonstrate the autonomous grid reconfiguration using the smart breaker. As shown in Fig. 2, it is divided into three sections each of which has a GFM resource using dVOC rated at 10 MVA with local loads with two breakers. The local loads are scaled to demonstrate the reconfiguration of unevenly loaded inverter resources. By the autonomous operation of the breakers, they will be combined into an interconnected system. Another breaker located at bus #7 emulates the autonomous load recovery. The voltage difference-based method is used for restoring the system shown in Fig. 2.

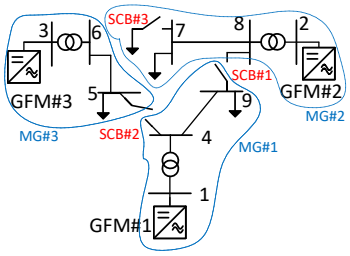

Fig. 2: 9-bus system with 3 GFMs and 3 SCBs.

Another scenario shown in Fig. 3, where a microgrid including five GFM inverters divided in four sections operating in droop-based control is used. Each of these inverters has a corresponding load. In addition, there is a short-circuit fault in the network as well as a large load which cannot be powered by any single inverter. Five SCBs are present to manage the grid restoration. At initial start-up, all the SCBs are all open. After the restoration process has completed, all five inverters will be operating in parallel and the heavy load will be finally recovered. The short-circuit will be correctly identified by the SCB and not connected to the microgrid.

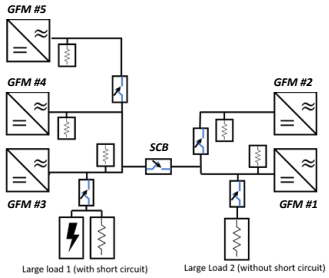

Fig. 3: Microgrid consisting of GFMs, SCBs, loads and faults.

B. Hardware Testbed

The hardware testbed comprises programmable inverters (TAPAS), loads, and a relay-driven switch. TAPAS developed by Siemens Technology [11] is a "Software Defined Inverter" (SDI) developed from a Siemens start-up. Specifications are listed in Table II. As illustrated in Fig. 4, two microgrids are implemented with a breaker in between. Each microgrid is formed by six grid forming inverters with a star-connected static load (baseline) and a controllable RLC load (for transients), as depicted in the single line diagram in Fig. 4. A BeagleBone board with RIAPS is assigned per inverter and controllable load to record the measurements and to implement a load profile, respectively. In the hardware testbed, droop-based control is used. The SCB is implemented with a 4-channel relay module with the PLL-based control logic as displayed in Fig 5. The hardware details are summarized in Table II.

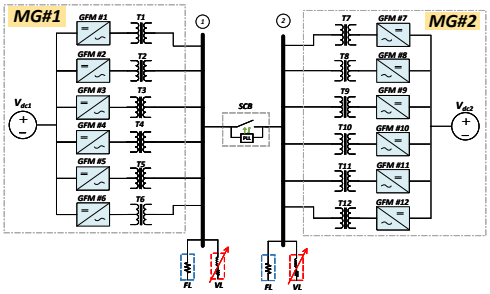

Fig. 4: One line diagram of 2-bus system for hardware experiments, containing 12-GFMs with a smart circuit breaker.

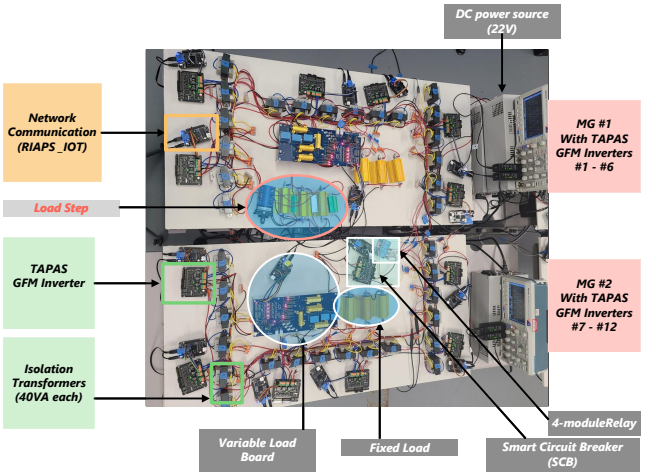

Fig. 5: Hardware testbed setup comprising the 12 droop-based inverters and circuit breaker as described in Table II.

TABLE II: Hardware System Components.

Components	Specifications
Grid-forming inverters	12 x TAPAS inverters w/ $22V_{DC}$ in, 8 V_{AC} out LC filter: 1.3 uH and 13.2 μF droop gains: 7% for LDG and 15% for HDG controller: Texas Instruments TMS320F28069M
Data acquisition	Beagle Bone Black with RIAPS
Isolation transformer	4000-60E07K999, 1:1 single phase, 3EA per inverter used for $\Delta - Y$ connection
Loads	~30 W for MG#1, ~10 W for MG#2 (basecase)
Smart circuit breaker	ELEGOO 4 Channel 5VDC Relay Module

IV. Results and Discussion

This section provides results from the software and hardware testbeds and discussion.

A. Simulation Results

From the software testbed developed, shown in Fig. 2, the inverter-driven black start and grid reconfiguration are demonstrated. The test case presents a scenario where the system is in blackout and divided into three sections with

all breakers open. The entire process, from the inverter blackstart to the full restoration, is captured in Fig. 6.

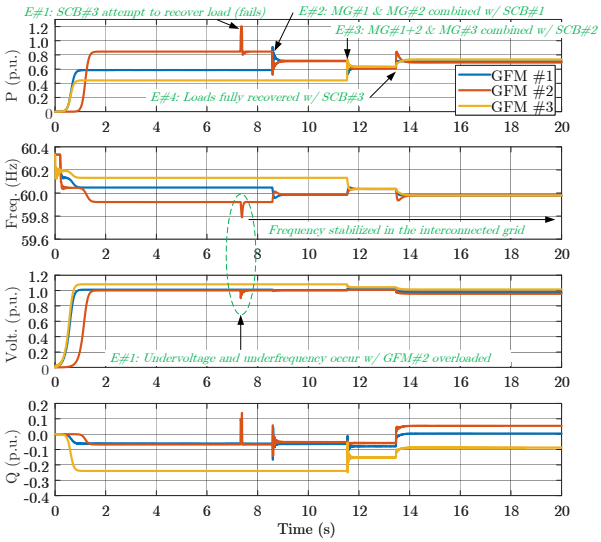

Fig. 6: Simulation result of black start and grid reconfiguration with dVOC GFM inverters and the smart circuit breakers.

First, the GFM inverters blackstart, gradually ramping up the voltage to suppress the inrush during cold load pick up (see [9] for details), and resulting in three islanded grids (refer Fig. 2 for notations) with individually loaded and thus system variables deviated each other. As it identifies the voltage recovered, at around 7 seconds, SCB #3 attempts to recover the local load at Bus #7; however, it reopens because it causes overloading and under-frequency ($E\#1$). At 8.5 seconds, SCB #1 successfully combines MG #1 and MG #2 without severe transients ($E\#2$) as discussed in Section III. Following, at 11.5 seconds, SCB #2 interconnects MG #3 with the combined system ($E\#3$). The second attempt of SCB #3 to recover the load remaining is successful as the interconnected grid now has increased generation ($E\#4$). As shown, the entire process executes without human intervention, autonomously, to facilitate the swift system restoration: the three inverter microgrids autonomously black start, and the GFM resources collectively stabilize the frequency and voltage as combined, with the circuit breakers gradually interconnecting the critical boundaries with local measurements, increasing reliability.

In Fig. 7, we describe the restoration of the microgrid depicted in Fig. 3. At initial start-up, all the SCBs are open, and GFM $\#2 - \#4$ are on. GFM #1 switches on shortly after start-up. GFM #5 switches on after 9 seconds. Following start-up, each of the five SCBs acts to connect the different components of the network together. The detailed restoration sequence for the microgrid is shown in Table III.

B. Hardware Testbed Results

The parallel operation of GFM inverters is shown in Figs. 8 and 9. The six GFM inverters in each microgrid are

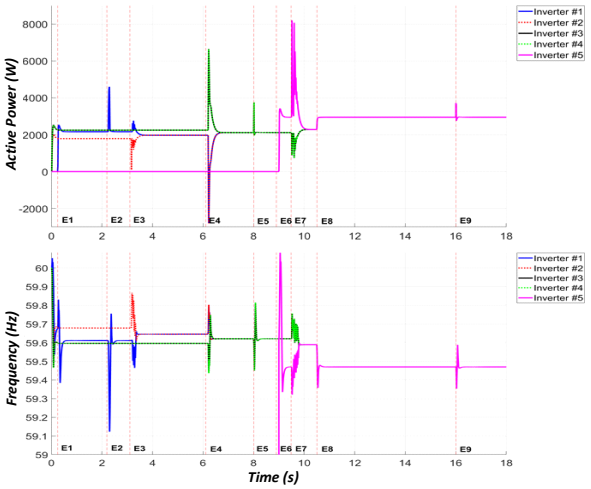

Fig. 7: Inverter active power and frequency during restoration for microgrid shown in Fig. 3.

TABLE III: Microgrid Restoration Sequence.

Event Number	Approx. Time(s)	Event Description
E1	t=0&0.4	GFMs #2 - #4 switch on at t=0. GFM #1 switches on at t=0.4.
E2	t=2.3	SCB tries to connect large load 2 to GFM #1. SCB detects under frequency condition and disconnects. Reconnection will be attempted again after 10 seconds.
E3	t=3	SCB separating GFM #1 and GFM #2 connects after sufficient time has lapsed and frequency difference between inverters are below threshold.
E4	t=6	SCB separating GFM #1 /GFM #2 and GFM #3 / GFM #4 connects after sufficient time has lapsed and frequency difference between two pairs of inverters is below threshold.
E5	t=8	SCB tries to connect large load1 to GFM #1-#4. SCB detects short circuit condition and disconnects.
E6	t=9	GFM#5 switches on at t=9.0.
E7	t=9.5	SCB separating GFM #5 and GFM #4 connects after sufficient time has lapsed and frequency difference between inverters is below threshold.
E8	t=10.5	SCB tries to re-connect large load 2 (from E2) to GFMs #1-#5. SCB does not detect an under-frequency condition, so connection is successful.
E9	t=16	SCB tries to connect large load 1 to GFM #1-#5. SCB detects short circuit condition and disconnects.

operating under a Low Droop Gain (LDG) share the active power set-points. A time delay of 20 seconds is present between successive events on MG#1 & MG#2. As shown in Fig. 8, Inverters $1-6$ (plotted in dashed lines) establish MG#1, starting from ~30W at (t=0s). Similarly, Inverters $7-12$ (plotted in solid lines) black starts MG#2, starting at a different operating point of ~10 W at (t=128s).

Fig. 9 depicts the voltage and reactive power of the GFM inverters operating under LDG. The inverters are able to collectively regulate the voltage around the nominal value after they are successively turned on, and the moderate reactive power sharing among the inverters is achieved. The SCB operation can be noted at (t=262s), where MG#1 and MG#2, initially islanded operating at different loadings, combine and operate at a common operating point, evenly sharing the total load. Successively, a load step is introduced at (t=265s), as observed in Figs. 8 and 9. The MGs combine into a single MG and responds to the load step successfully, and upon load removal, the microgrids return to their individual operating points.

Another scenario comprising of the reconfiguration se-

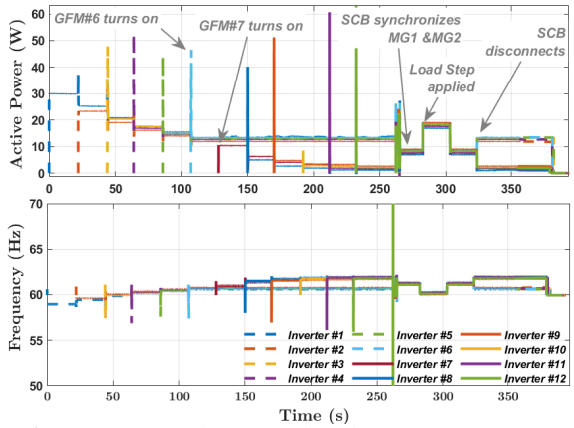

Fig. 8: Active power and frequency of 12-GFMs parallel operation (with LDG) in the hardware testbed, shown in Fig. 5.

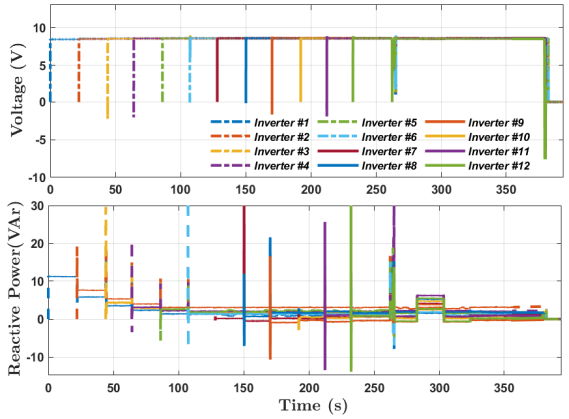

Fig. 9: Reactive power and voltage of 12-GFMs parallel operation (with LDG) in the hardware testbed, shown in Fig. 5.

quence with the relay status has been shown in Fig. 10 for a high droop gain (HDG) operation of MG#1 and MG#2. The SCB is able to synchronize the grid at (t=257s). The transient response of the MGs seen in the figure settles down when the relay is in the 'ON' status. With the manual disconnection of the breaker at (t=323s), the microgrids re-distribute their power sharing.

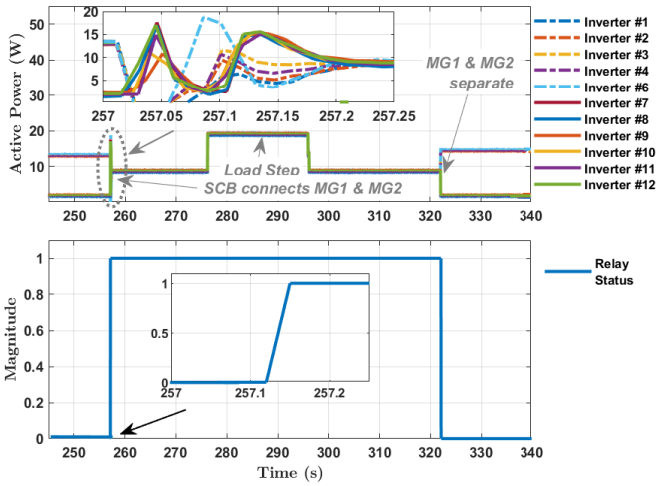

Fig. 10: Active power 12-GFMs parallel operation (with HDG) and SCB-based relay operation.

V. Conclusions

In this paper, a autonomous microgrid restoration using GFM inverters and SCBs has been proposed and demonstrated. Both droop-based and dVOC-based control strategies have been used for GFM inverters, which are programmed to autonomously black start a grid in blackout in this study. For smart breakers, intelligently combining individually energized microgrids and recovering loads with fault and overload detection capability, two methods have been introduced, compared, and demonstrated. This study has demonstrated the autonomous black start and system restoration concept in software and hardware testbeds. In the two software simulations, the modified IEEE-9 bus system and custom 5-GFM inverter microgrid, initially split in small microgrids, are black-started by GFM inverters and recombined with SCBs without communication or human intervention. In addition, two microgrid system restoration and power sharing performance with different droop gains has been demonstrated in the hardware experiments with 12 GFM inverters, 1 SCB, and controllable loads to evaluate the feasibility.

References

[1] C. Loutan, P. Klauer, S. Chowdhury, S. Hall, M. Morjaria, V. Chadliev, N. Milam, C. Milan, and V. Gevorgian, "Demonstration of essential reliability services by a 300-MW solar photovoltaic power plant," tech. rep., National Renewable Energy Lab.(NREL), Golden, CO (United States), 2017.

[2] Y. Lin, J. H. Eto, B. B. Johnson, J. D. Flicker, R. H. Lasseter, H. N. Villegas Pico, G.-S. Seo, B. J. Pierre, and A. Ellis, "Research roadmap on grid-forming inverters," tech. rep., National Renewable Energy Lab.(NREL), Golden, CO, USA, 2020.

[3] M. C. Chandorkar, D. M. Divan, and R. Adapa, "Control of parallel connected inverters in standalone ac supply systems," *IEEE Trans. Ind. Appl.*, vol. 29, no. 1, pp. 136–143, 1993.

[4] K. De Brabandere, "Voltage and frequency droop control in low voltage grids by distributed generators with inverter front-end," *Katholieke University Leuven, Leuven, Belgie*, 2006.

[5] B. B. Johnson, S. V. Dhople, A. O. Hamadeh, and P. T. Krein, "Synchronization of parallel single-phase inverters with virtual oscillator control," *IEEE Trans. Power Electron.*, vol. 29, no. 11, pp. 6124–6138, 2013.

[6] Y. Lin, G.-S. Seo, S. Vijayshankar, B. Johnson, and S. Dhople, "Impact of increased inverter penetration on power system small-signal stability," in *Proc. IEEE Power & Energy Society General Meetings*, 2021.

[7] G.-S. Seo, M. Colombino, I. Subotic, B. Johnson, D. Groß, and F. Dörfler, "Dispatchable virtual oscillator control for decentralized inverter-dominated power systems: Analysis and experiments," in *Proc. IEEE Applied Power Electron. Conf.*, pp. 561–566, 2019.

[8] M. Braun, J. Brombach, C. Hachmann, D. Lafferte, A. Klingmann, W. Heckmann, F. Welck, D. Lohmeier, and H. Becker, "The future of power system restoration: Using distributed energy resources as a force to get back online," *IEEE Power Energy Mag.*, vol. 16, no. 6, pp. 30–41, 2018.

[9] H. Jain, G.-S. Seo, E. Lockhart, V. Gevorgian, and B. Kroposki, "Blackstart of power grids with inverter-based resources," in *Proc. IEEE Power & Energy Society General Meetings*, pp. 1–5, 2020.

[10] A. Tayyebi, D. Groß, and A. Anta, "Grid forming converters: Implementation of grid-forming control techniques in ieee 9-bus system," 2019.

[11] SIEMENS, "Sdi-softwaredefinedinverter/tapas." https://github.com/SDI-SoftwareDefinedInverter/TAPAS.